

# **Volumetric–Densimetric Measurements of the Adsorption Equilibria of Binary Gas Mixtures**

*J.U. Keller, N. Iossifova and W. Zimmermann*

*Reprinted from*

## **Adsorption Science & Technology**

2005 Volume 23 Number 9

*Multi-Science Publishing Co. Ltd.  
5 Wates Way, Brentwood, Essex CM15 9TB, United Kingdom*

## Invited Contribution

---

### Volumetric–Densimetric Measurements of the Adsorption Equilibria of Binary Gas Mixtures

J.U. Keller\*, N. Iossifova and W. Zimmermann *Institute of Fluid- and Thermodynamics, University of Siegen, 57068 Siegen, Germany.*

(Received 26 October 2004; revised form accepted 3 June 2005)

**ABSTRACT:** A new method for measuring the binary co-adsorption equilibria of gas mixtures with non-isomeric components on porous solids such as activated carbons or zeolites is proposed. The method does not require an analysis of the sorptive gas phase in adsorption equilibrium and can be automated fairly simply. It consists of a simple volumetric/manometric gas expansion arrangement combined with the measurement of the density of the sorptive gas mixture in equilibrium via the buoyancy of a sinker fixed to a microbalance. These gas density measurements can be performed on-line preferably with a magnetic suspension balance (MSB) (Rubotherm GmbH, Bochum, Germany, 2-site-type).

The experimental lay-out of the instrument used is given and the measurement procedure is outlined. The theory of the measurement is presented and expressions for experimental uncertainties of component masses adsorbed are provided. As examples, the co-adsorption equilibria data of gas mixtures ( $\text{CO}_2/\text{CH}_4$ ) and ( $\text{H}_2/\text{CH}_4$ ) on activated carbon (D47/3, CarboTech, Essen, Germany) at 293 K and 333 K for pressures up to 2 MPa are presented and discussed to a certain extent.

## INTRODUCTION

Most gas separation processes based on adsorption on highly porous solids which are used today utilize equilibria effects, i.e. the selectivity of one component against the other in adsorption equilibria loads at a given pressure, temperature and concentration of the sorptive gas mixture (Basmadjian 1996; Kast 1988; Ruthven *et al.* 1994; Yang 1997). Hence, for the proper design of gas separation processes by selective adsorption, such as air separation ( $\text{N}_2$ ,  $\text{O}_2$ ), the cleaning of natural gas ( $\text{CH}_4$ ,  $\text{H}_2\text{S}$ ) or the upgrading of low-energy flue gas ( $\text{CH}_4$ ,  $\text{N}_2$ ,  $\text{CO}_2$ ), etc., the binary co-adsorption equilibria data of the respective components should be known. In principle, approximate data for these equilibria can be gained from purely gravimetric or volumetric measurements. However, as these only give the sum of the masses of both adsorbed components, model assumptions on the structure of the binary adsorbate are needed in addition, in order to calculate the masses of the separate single components.

An early step in this direction was proposed by van Ness (1969) based on the Gibbs adsorption isotherm model (Ruthven *et al.* 1994; Beutekamp 2002). However, the resulting data were not

\*Author to whom all correspondence should be addressed. E-mail: keller@ift.maschinenbau.uni-siegen.de.

always reliable and of sufficient accuracy. Also, as it is still not possible to calculate accurate co-adsorption equilibria data *ab initio*, nor even from the adsorption data for the pure components and the (normally scarce) information regarding the sorbent material, there was a growing need for experimental methods to measure these quantities. Several methods are now available (Keller and Staudt 2004). The intention behind this paper is to inform the reader interested in the experimental determination of co-adsorption equilibria of binary gas mixtures on porous solids, such as activated carbons or zeolites, of a new measurement method which does not need a gas chromatograph. This method combines volumetric/manometric measurements and gas density or densimetric measurements using buoyancy effects. In this way, it is possible to determine the masses of both adsorbed components without the need to analyze the sorptive gas using a gas chromatograph or a mass spectrometer.

Experimental information regarding the instrument and the measurement procedure is given in the next section. The measurement theory is outlined and formulae provided regarding the experimental uncertainties of the adsorbed component masses. Finally, as an example, volumetric–densimetric measurements for pure methane (CH<sub>4</sub>), carbon dioxide (CO<sub>2</sub>) and hydrogen (H<sub>2</sub>) and certain of their binary mixtures measured at 293 K and 333 K for pressures up to 2 MPa are presented and discussed to a certain extent.

## INSTALLATION

A schematic diagram of an installation which may be employed to obtain volumetric–densimetric measurements is depicted in Figure 1, while Figure 2 presents a photograph of such an instrument which has been designed and built in our laboratory (IFT PB A 0126/1). The instrument mainly consists on an adsorption chamber (volume,  $V_{AC}$ ) which includes the sorbent sample and a magnetic suspension balance (MSB) with only two working positions bearing a sinker (titanium) for gas density measurements (Rubotherm GmbH, Bochum, Germany). In addition, there are storage vessels (volumes,  $V_{SV1}$ ,  $V_{SV2}$ ) for the pure sorptive gas components and auxiliary equipment such as a gas circulation pump, valves, manometers and thermometers, a vacuum pump and a gas-supply system. All vessels and tubes connecting these various components should be thermostatted.

For pressures above ambient, all vessels and tubes should be manufactured in stainless steel with internal surfaces being electropolished or, preferably, gilded. For pressures below ambient, i.e. vacuum systems, the corresponding components may be constructed in glass. Sealing materials should be chosen according to the sorptive gases to be studied and the ranges of temperature and pressure to be employed. For corrosive gases and high pressures, the use of metallic sealings (such as silver or steel) is always recommended. The adsorption chamber includes a sample of sorbent material of mass  $m^s$ , which should have been “activated” prior to measurement by heating at higher temperatures and in a vacuum for several hours to reduce the amount of pre-adsorbed molecules. Standard procedures for activation have been described by a number of authors, e.g. Rouquerol *et al.* (1999), Keller *et al.* (1999) and Staudt (2000). The so-called helium volume ( $V_{He}^s$ ) of the sorbent sample should also be known. If not, it has to be determined by a helium gas expansion experiment as follows. The installation is evacuated ( $p < 10$  Pa) and one or both of the storage vessels filled with a known amount of helium gas ( $m_{He}^*$ ) (quality > 99.9990%  $\equiv$  5.0). The valves to the adsorption chamber are then opened allowing the helium gas to expand and to be partly adsorbed or absorbed in the sorbent material sample. This process may last milliseconds, minutes or — in the case of highly activated carbon — hours or days (Keller and Staudt 2004). After thermodynamic equilibrium has been attained, i.e. constancy of pressure ( $p$ ) and

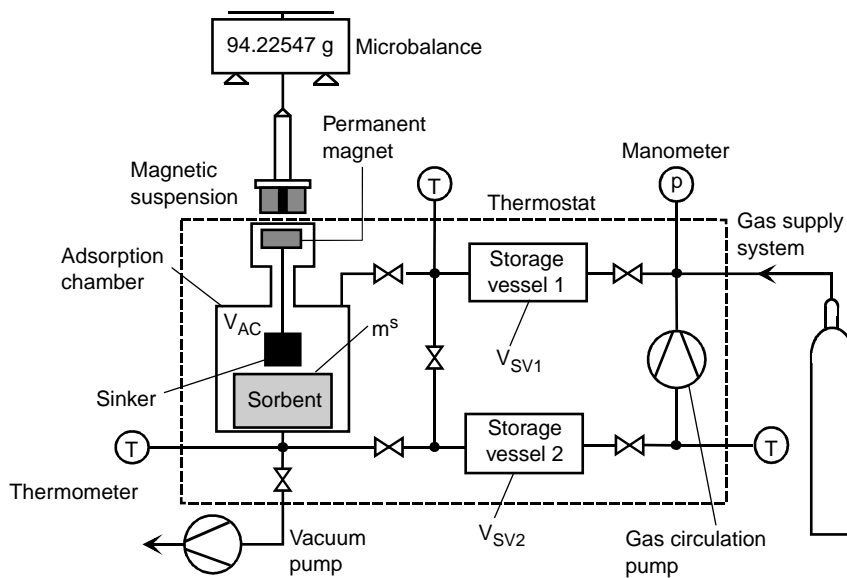


**Figure 1.** Instrument for volumetric–densimetric measurements of binary co-adsorption equilibria of gas mixtures on porous solids without using a gas chromatograph. The sorptive gas prepared in the system is assumed to be a binary mixture with known initial molar concentrations ( $y_1^*$ ,  $y_2^*$ ). © IFT University of Siegen, 2002.



**Figure 2.** Instrument for volumetric–densimetric measurements of binary co-adsorption equilibria of gas mixtures on porous solids without using a gas chromatograph. The magnetic suspension balance, cf. Figure 1, near the centre is complemented by a thermostat at left, an electronic unit for automated measurements and control in the rear, a PC monitor at right and a helium gas-based instrument for leak detection in the foreground at right. © IFT University of Siegen, 2002.

temperature (T) in the installation has been realized, the density of the helium gas ( $\rho_{\text{He}}^f$ ) can be determined from the MSB. The volume of sorbent material ( $m^s$ ) which is not capable of penetration by the helium molecules can be calculated from the mass balance of the helium gas via the relationship:

$$m_{\text{He}}^* = m_{\text{He}}^a + \rho_{\text{He}}^f (V_{\text{AC}} + V_{\text{SV1}} + V_{\text{SV2}} + \Delta V - V_{\text{He}}^s) \quad (1)$$

assuming that the mass of helium adsorbed may be neglected in comparison to the mass of helium in the gaseous phase, i.e.  $m_{\text{He}}^a = 0$ :

$$V_{\text{He}}^s = \frac{m_{\text{He}}^*}{\rho_{\text{He}}^f} - (V_{\text{AC}} + V_{\text{SV1}} + V_{\text{SV2}} + \Delta V) \quad (2)$$

The quantity  $\Delta V$  in equations (1) and (2) corresponds to the volume of tubes and valves filled with helium gas. This quantity is best determined by calibration experiments, i.e. gas expansion without a sorbent material in the adsorption chamber.

To measure co-adsorption equilibria, one should proceed as follows. Pure gases of both components (1, 2) with masses ( $m_1^*$ ,  $m_2^*$ ) are prepared in the storage vessels ( $V_{\text{SV1}}$ ,  $V_{\text{SV2}}$ ). Alternatively, either one or both storage vessels are filled with a binary gas mixture with the total mass:

$$m^* = m_1^* + m_2^* \quad (3)$$

and known molar concentrations ( $y_1^*$ ,  $y_2^*$ ). Upon opening the expansion valves, the gas expands to the adsorption chamber where it is partly adsorbed on the (external and internal) surface of the sorbent material. For mixture adsorption, it is essential at this stage to turn on the gas circulation pump and to avoid concentration differences in the gas phase within the installation (and also to speed up the adsorption process). The gas should be (slowly) circulated until adsorption equilibrium is reached, i.e. the gas pressure (p) within the system and the signal from the microbalance ( $\Omega$ ) remain "constant" after stopping the gas circulator. In practice, this state often has to be defined in technical terms, i.e. by stating that the microbalance reading does not change more than a certain prescribed amount ( $\Delta\Omega$ ) within a certain period of time ( $\Delta t$ ). Such a state may be called a "technical equilibrium", which for  $\Delta t \rightarrow \infty$ , i.e.  $\Delta t > 1$  h and  $\Delta\Omega \rightarrow 0$ , i.e.  $\Delta\Omega < 10^{-6} |\Omega|$  tends to physical or exact thermodynamic equilibrium. We have experienced very rapid adsorption processes where equilibrium was attained within a few minutes, but also very slow ones which took days and even weeks to complete. One such example of the latter situation occurred with the penetration of helium into porous materials (Keller and Staudt 2004). Hence, it is a matter of practice to choose proper values of  $\Delta\Omega$  and  $\Delta t$  according to the nature and behaviour of the adsorption system and the accuracy of the data needed. From the recorded data ( $p^*$ , p, T,  $y_i^*$ ,  $i = 1, 2$ ,  $\Omega$ ), it is possible to calculate the masses of both components adsorbed ( $m_1^a$ ,  $m_2^a$ ) as will be outlined in the next section.

Naturally, a set of similar step-up experiments can be performed with increasing sorptive gas pressures (p) in the AC. However, account should be taken of the fact that the uncertainties associated with the results add up in such a procedure. For this reason, it is recommended that no more than, say, four sequential pressure-step experiments are conducted so that the uncertainties of the adsorbed masses and sorptive gas concentrations are kept below or at 10% (also see the next section).

**THEORY**

The masses of both components ( $i = 1, 2$ ) of the sorptive gas being adsorbed ( $m_1^a, m_2^a$ ) can be determined from the mass balances:

$$m_i^* = m_i^a + m_i^f, \quad i = 1, 2 \tag{4}$$

as follows. The masses of the gas components originally supplied ( $m_1^*, m_2^*$ ) can be calculated from:

- either the respective thermal equation of state (EOS), if pure components are prepared separately in the storage vessels

$$m_i^* = \frac{p_i^* V_{svi} M_i}{RTZ_{i0}(p_i^*, T)}, \quad i = 1, 2 \tag{5}$$

- or from the gas mixture EOS, if a mixture of known initial concentrations ( $y_1^*, y_2^*$ ) is supplied to the storage vessel(s):

$$m_i^* = \frac{y_i^* p^* V_{sv} M_i}{RTZ(p^*, T, y_1^*, y_2^*)}, \quad i = 1, 2 \tag{6}$$

In equation (5),  $p_i^*$  is the gas pressure in the storage vessel  $i$ ,  $M_i$  the molecular mass of component  $i$ ,  $R$  is the universal gas constant,  $T$  the absolute temperature at which the adsorption experiment is performed and  $Z_{i0} = Z_{i0}(p_i^*, T)$  is the real gas factor or the so-called compressibility of pure component  $i$ . For many (industrially relevant) gases, this factor can be considered as a known function of the gas pressure ( $p_i^*$ ) and the temperature ( $T$ ) (Sengers *et al.* 2000a; Reid *et al.* 1983).

Similarly, in equation (6), the function  $Z = Z(p^*, T, y_1^*, y_2^*)$  is the real gas factor of the sorptive gas mixture (1, 2) (Sengers *et al.* 2000b). Nowadays, this quantity is also well known for many binary gas mixtures. If not, it can actually be measured by a simple expansion and mixture experiment of the pure gas components in the installation (Figure 1), which is performed prior to the adsorption experiment.

The masses of the sorptive gas components in adsorption equilibrium ( $m_i^f, i = 1, 2$ ) included in equation (4) can be calculated from gas density measurements using the buoyancy of a sinker coupled to the magnetic suspension balance, i.e. via the equation:

$$\Omega = m_{si} - \rho^f V_{si} \tag{7}$$

Here  $\Omega$  is a measured quantity which comes from the microbalance readings, while  $m_{si}$  and  $V_{si}$  correspond to the mass and volume of the sinker. As the density of the sorptive gas ( $\rho^f$ ) is now a known quantity, the extensivity relationship of the sorptive gas masses:

$$m_1^f + m_2^f = \rho^f V^f \tag{8}$$

with the gas volume ( $V^f$ ) given by:

$$V^f = V_{AC} + V_{SV1} + V_{SV2} + \Delta V - V_{AS} \quad (9)$$

$$\equiv V^* - V^{as} \quad (9.1)$$

where  $V^{as}$  corresponds to the volume of the combined sorbent (s) and adsorbate (a) system seen by the sorptive gas molecules and approximated by the helium volume of the sorbent material, i.e.  $V^{as} \equiv V_{He}^s$  [cf. equation (2)], provides an algebraic equation for  $(m_1^f, m_2^f)$ . It can be coupled with the EOS of the sorptive gas:

$$\frac{m_1^f}{M_1} + \frac{m_2^f}{M_2} = \frac{pV^f}{RTZ(p, T, y_i)} \quad (10)$$

Solving equations (8)–(10) for  $(m_1^f, m_2^f)$  we get:

$$m_1^f = \frac{M_1}{M_1 - M_2} \left( \rho^f - \frac{pM_2}{RTZ(p, T, y_1, y_2)} \right) V^f \quad (11.1)$$

$$\equiv \rho_1^f V^f \quad (11.1.1)$$

$$m_2^f = \frac{M_2}{M_2 - M_1} \left( \rho^f - \frac{pM_1}{RTZ(p, T, y_1, y_2)} \right) V^f \quad (11.2)$$

$$\equiv \rho_2^f V^f \quad (11.2.1)$$

Equations (11) still include the unknown molar concentrations,  $y_1, y_2$ , of the sorptive gas. These quantities have to be calculated from the respective mass concentrations,  $w_1, w_2$ , via:

$$y_i = \frac{w_i/M_i}{(w_1/M_1) + (w_2/M_2)}, \quad i = 1, 2 \quad (12)$$

$$w_i = \frac{m_i^f}{m_1^f + m_2^f}, \quad i = 1, 2 \quad (12.1)$$

The mass concentrations can be calculated iteratively from the EOS, [equation (10)], and the normalization condition:

$$w_1 + w_2 = 1 \quad (13)$$

as the density of the sorptive gas ( $\rho^f$ ) is known. Combining equations (10) and (13) we get:

$$w_1 = \frac{M_1 M_2}{M_2 - M_1} \left( \frac{p}{\rho^f RTZ(p, T, w_1)} - \frac{1}{M_2} \right) \quad (14.1)$$

$$w_2 = \frac{M_1 M_2}{M_1 - M_2} \left( \frac{p}{\rho^f RTZ(p, T, w_2)} - \frac{1}{M_1} \right) \quad (14.2)$$

Starting with the ideal gas value of the compressibility factor ( $Z = 1$ ), equations (14) lead to certain mass fractions ( $w_{i1}$ ,  $i = 1, 2$ ) which can be inserted into an analytic expression for  $Z = Z(p, T, w_i)$ . Equations (14) can also be iterated to converge (usually after ca. five steps) to the sorptive gas mass fractions ( $w_i$ ,  $i = 1, 2$ ). Then from equation (4) combined with equations (5) and (11), the Gibbs excess masses of both adsorbed components can be calculated as:

$$m_{1GE}^a = \frac{p_1^* V_{SV1} M_1}{RTZ_{10}^*(p_1^*, T)} - \frac{M_1}{M_1 - M_2} \left( \rho^f - \frac{pM_2}{RTZ(p, T, w_1)} \right) \cdot (V^* - V_{He}^s) \quad (15.1)$$

$$m_{2GE}^a = \frac{p_2^* V_{SV2} M_2}{RTZ_{20}^*(p_2^*, T)} - \frac{M_2}{M_2 - M_1} \left( \rho^f - \frac{pM_1}{RTZ(p, T, w_2)} \right) \cdot (V^* - V_{He}^s) \quad (15.2)$$

Here, according to equation (9), the volume of the sorptive gas phase ( $V^f$ ) has been chosen as:

$$V^f = V^* - V_{He}^s \quad (16)$$

with the abbreviation

$$V^* \equiv V_{AC} + V_{SV1} + V_{SV2} + \Delta V \quad (17)$$

and  $V_{He}^s$  being an approximation for the sorbent volume ( $V^s \equiv V_{He}^s$ ).

If the so-called absolute masses adsorbed ( $m_1^a, m_2^a$ ) are needed instead of the Gibbs excess masses, the volume of the combined sorbent/sorbate phase ( $V^{as}$ ) in the sorptive gas volume [equation (9a)] should be approximated by:

$$V^{as} = V_{He}^s + \frac{m_1^a}{\rho_{10}^*} + \frac{m_2^a}{\rho_{20}^*} \quad (18)$$

Here ( $\rho_{10}^*, \rho_{20}^*$ ) are the densities of the pure components (1, 2) in a reference liquid state, e.g. the liquid triple state of the pure fluids (Keller and Staudt 2004). Combining the mass balances [equation (4)] with equations (5), (11), (16) and (18), we obtain two linear equations for ( $m_1^a, m_2^a$ ) that can easily be solved to yield:

$$m_1^a = \frac{1}{D} \left[ \left( 1 - \frac{\rho_2^f}{\rho_{20}^*} \right) m_1^* + \frac{\rho_1^f}{\rho_{20}^*} m_2^* - \rho_1^f (V^* - V_{He}^s) \right] \quad (19.1)$$

$$m_2^a = \frac{1}{D} \left[ \left( 1 - \frac{\rho_1^f}{\rho_{10}^*} \right) m_1^* + \frac{\rho_1^f}{\rho_{10}^*} m_2^* - \rho_2^f (V^* - V_{He}^s) \right] \quad (19.2)$$

with

$$D = 1 - \frac{\rho_1^f}{\rho_{10}^*} - \frac{\rho_2^f}{\rho_{20}^*} \quad (20)$$

The partial densities of the sorptive gas ( $\rho_1^f, \rho_2^f$ ) are given by equations (11) and (11a), and the total masses of gas originally supplied ( $m_1^*, m_2^*$ ) by either equation (5) or (6). It should be noted that for isomeric gas components, e.g. CO/N<sub>2</sub> mixtures, formulae (11) and hence equations (14), (15) and (19) are inapplicable since the starting system of algebraic equations (4), (8) and (10) becomes algebraically dependent in this case. The volumetric–densimetric method fails for such gas mixtures; instead, binary co-adsorption equilibria require analysis of the gas phase, i.e. the determination of respective sorptive gas concentrations ( $w_1, w_2$  or  $y_1, y_2$ ). Also, it should be noted that for pure gases ( $i = 2, N = 1$ ), volumetric–densimetric measurements allow the determination of adsorption equilibria without the need to use a thermal equation of state for the sorptive gas, cf. equations (4), (5), (7) and (8).

For the sake of completeness, we also mention the dispersion or uncertainty of the Gibbs excess masses  $m_{iGE}^a, i = 1, 2$ , as given by equation (15). Gauss' law of uncertainty propagation leads to the expression:

$$\begin{aligned} \sigma_{miGE}^* = & \left( \frac{V_{SV} M_i}{RTZ_{i0}^*} \right)^2 \sigma_{P_i^*}^2 + \left( \frac{P_i^* M_i}{RTZ_{i0}^*} \right)^2 \sigma_{V_{SV}}^2 + \left( \frac{P_i^* V_{SV}}{RT^2 Z^*} M_i \right)^2 \sigma_T^2 + \left( \frac{P_i^* V_{SVi}}{RTZ_{i0}^*} M_i \right)^2 \sigma_{Z_{i0}}^2 + \\ & \left( \frac{M_i}{M_i - M_{i+1}} \right)^2 (V^* - V_{He}^s)^2 \left[ \left( \sigma_{\rho^f}^2 + \frac{M_{i+1}}{RTZ} \right)^2 \sigma_P^2 + \right. \\ & \left. \left( \frac{pM_{i+1}}{RT^2 Z} \right)^2 \sigma_T^2 + \left( \frac{pM_{i+1}}{RTZ^2} \right)^2 \sigma_Z^2 \right] + \\ & \left( \frac{M_i}{M_i - M_{i+1}} \right)^2 \left( \rho^f - \frac{pM_{i+1}}{RTZ} \right)^2 (\sigma_{V^*}^2 + \sigma_{V_{SHe}}^2) \quad i = 1, 2 \end{aligned} \quad (21)$$

$$\sigma_{zi0}^2 = \left( \frac{\partial Z_{ip}}{\partial T} \right)^2 \sigma_T^2 + \left( \frac{\partial Z_{i0}}{\partial p_i^*} \right)^2 \sigma_{P_i^*}^2 \quad (22)$$

$$\sigma_Z^2 = \left( \frac{\partial Z}{\partial T} \right)^2 \sigma_T^2 + \left( \frac{\partial Z}{\partial p} \right)^2 \sigma_p^2 + O(\sigma_{yi}^2, i = 1, 2) \quad (23)$$

Here, the symbol  $O(\sigma_{yi}^2 \dots)$  indicates terms of order  $(\sigma_{yi}^2)$  which can often be neglected. The dispersions used in equation (21) are related to the respective measurable quantities as given in the scheme below.

Numerical examples readily show that in order to get accurate masses of the components of the adsorbate ( $m_{iGE}^a, i = 1, 2$ ), it is essential to have precise measurements of the system pressure ( $\sigma_p$ ) and temperature ( $\sigma_T$ ) to hand. Also, as already mentioned, the molar masses ( $M_1, M_2$ ) of the sorptive gas components should be “fairly different”, i.e.  $|M_2 - M_1| \geq 0.25 \text{Min}(M_1, M_2)$ . If this condition does not hold, the uncertainties expressed in equation (21) may well exceed 10%. Again, in this case, additional measurements of the sorptive gas concentrations in the equilibrium state considered are necessary. Typical numerical values of the relative uncertainties ( $\sigma_x/x$ ) of the various physical quantities  $x = p_i^*, V_{SVi}, T \dots$  are also given below.

x	$p_i^*$	$V_{SVi}$	T	$Z_i^*$	$\rho^f$	p	Z	$V^*$	$V_{He}^s$
$\sigma_x$	$\sigma_{p_i^*}$	$\sigma_{V_{SVi}}$	$\sigma_T$	$\sigma_{Z_i^*}$	$\sigma_{\rho^f}$	$\sigma_p$	$\sigma_z$	$\sigma_{V^*}$	$\sigma_{V_{He}^s}$
$ \sigma_x/x $	$10^{-4}$	$10^{-4}$	$10^{-3}$	$10^{-3}$	$10^{-3}$	$10^{-4}$	$10^{-3}$	$10^{-4}$	$10^{-3}$

If these uncertainties are available, then according to equation (21), the relative dispersions of the Gibbs excess masses adsorbed ( $\sigma_{miGE} / m_{iGE}^a$ ) will be  $\approx 10^{-2}$ ,  $i = 1, 2$ .

**EXPERIMENTAL**

Volumetric–densimetric measurements (VDMs) have been performed to determine the binary co-adsorption equilibria of the gas mixtures CO<sub>2</sub> + CH<sub>4</sub> and H<sub>2</sub> + CH<sub>4</sub> (Iossifova 2006) on activated carbon D47/3 (CarboTech, Essen, Germany) at T = 293 K and T = 333 K for pressures up to 2 MPa. Data for the adsorption equilibria of the pure gases and of the gas mixtures are presented below.

**Materials**

*Adsorbent*

Activated carbon AC D47/3, a mainly microporous substance, is used preferentially for the purification processes of methane and hydrogen. Some characteristic data for this material are listed in Table 1 and are followed by:

- a mercury intrusion diagram (Figure 3), taken at BAM, Berlin in September 2001 using a P 4000 porosimeter;
- the nitrogen adsorption isotherm measured at 77 K (Figure 4), taken in our laboratory in 2001;
- the integral and the differential pore volume distributions calculated from the data of Figure 4 by the BJH method (Yang 2003) [Figure 5(a) and (b)].

The curves in Figure 3 represent the intrusion and (irreversible) extrusion process data arising from the penetration of mercury into the carbon. As can be seen, the sorbent material employed

**TABLE 1.** Characteristics of Activated Carbon D47/3 (CarboTech, Essen, Germany)

<b>Mercury intrusion experiment</b>	
Total cumulative volume	455.26 mm <sup>3</sup> /g
Total specific surface area	57.80 m <sup>2</sup> /g
Average meso- and macro-pore diameter	6.42 μm
Total porosity	36.40%
Bulk density	0.7996 g/cm <sup>3</sup>
Apparent density	1.257 g/cm <sup>3</sup>
<b>Nitrogen adsorption isotherm at 77 K (BJH method)</b>	
BET surface area	951 m <sup>2</sup> /g

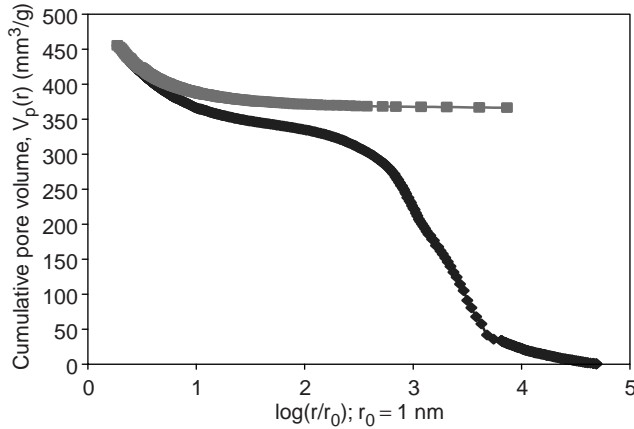


**Figure 3.** Cumulative or integral pore volume  $V_p(r)$  per unit mass of activated carbon D47/3 (CarboTech, Essen, Germany) measured at 293 K (mercury intrusion) as a function of the pore radius ( $r$ ) (Iossifova 2006). Data points correspond to the following:  $\blacklozenge$ , intrusion;  $\blacksquare$ , extrusion.

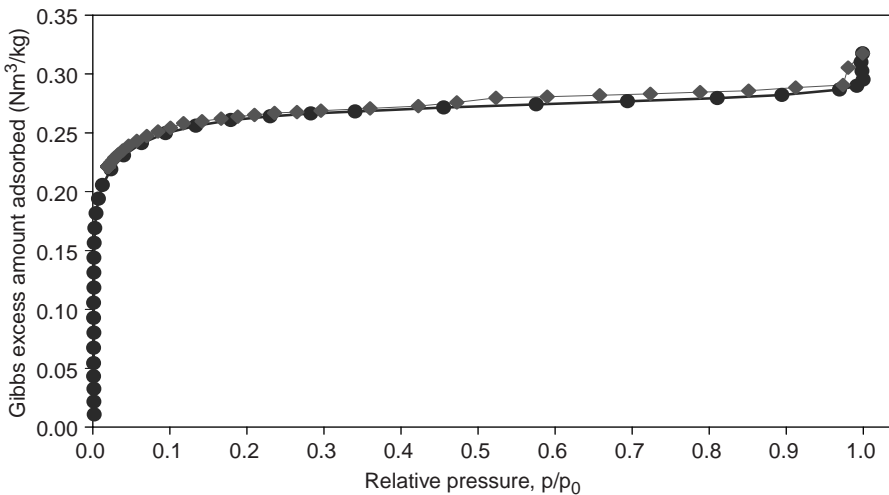


**Figure 4.** Adsorption/desorption isotherm of nitrogen ( $N_2$ , 5.0) on activated carbon D47/3 (CarboTech, Essen, Germany) ( $S_{BET} = 951 \text{ m}^2/\text{g}$ ) at 77 K,  $p_0 = 1 \text{ atm}$  (Iossifova 2006). Data points correspond to the following:  $\bullet$ , adsorption;  $\blacklozenge$ , desorption.

possessed some macropores ( $r > 25 \text{ nm}$ ,  $\log(r/r_0) > 1.4$ ,  $r_0 = 1 \text{ nm}$ ), especially in the micrometer range, but only a few mesopores ( $1 \text{ nm} < r < 25 \text{ nm}$ ,  $0 < \log(r/r_0) < 1.4$ ). This is confirmed by the results of the nitrogen adsorption/desorption measurements at 77 K for pressures  $p < 1 \text{ atm}$  shown in Figure 4 and the respective pore volume distributions calculated from these data by the BJH method (Yang 2003). For the sake of clarity, the mesopore section ( $1 \text{ nm} < r < 25 \text{ nm}$ ) in Figure 5(a) has been enlarged and is depicted in greater detail in Figure 5(b). The shapes of the curves were influenced considerably by the pre-adsorption of gases onto the carbon, i.e. on the activation procedure employed (evacuation for 2 h, helium at 373 K for 4 h and again evacuation and

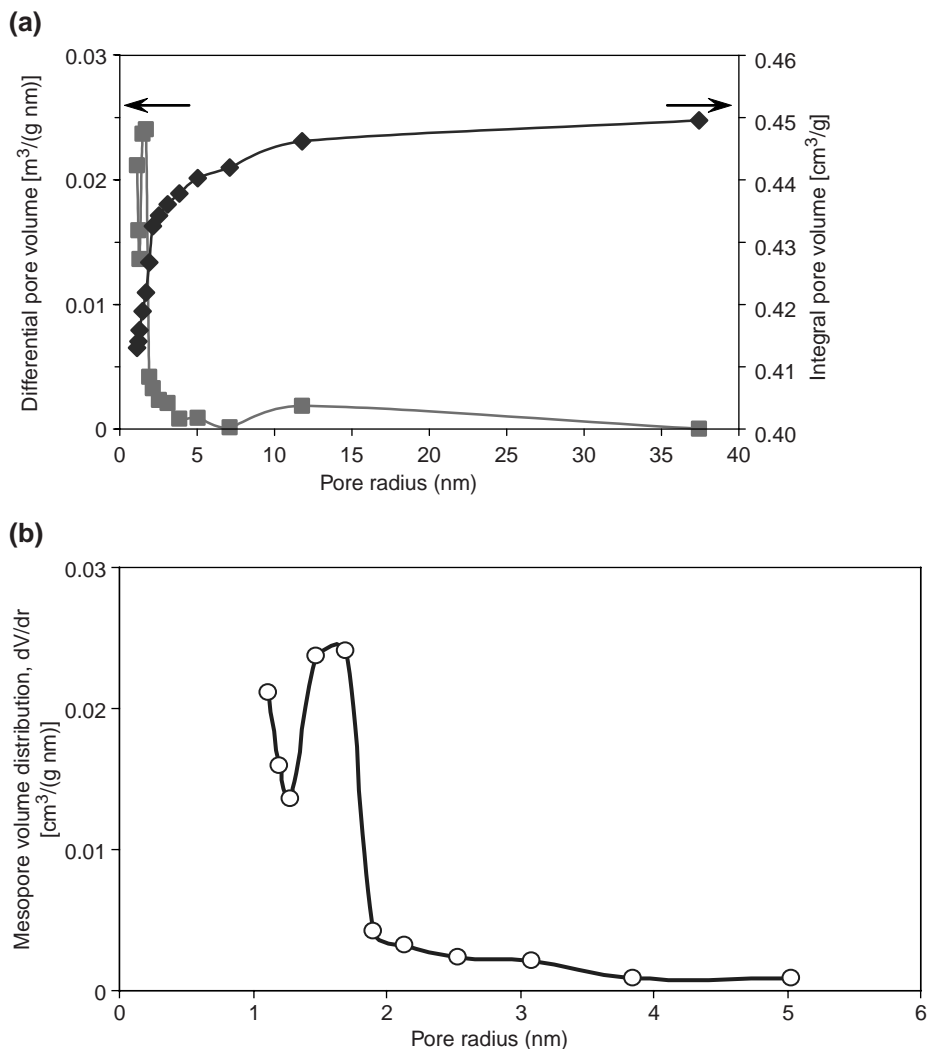


**Figure 5.** (a) Pore volume distribution function and (b) mesopore volume distribution function of activated carbon D47/3 (CarboTech, Essen, Germany) as calculated from the  $\text{N}_2$  adsorption isotherm of Figure 4 by the BJH method (Yang 2003).

cooling down to 298 K for several hours), but otherwise exhibited typical structures (Keller and Staudt 2004).

### Gases

The pure sorptive gases were supplied by Messer Griesheim, Düsseldorf, Germany with gas mixtures being produced directly in the experimental installation (Figures 1 and 2). The purities of the gases employed are listed in Table 2. The impurities in helium ( $\text{He}$ ) were mainly nitrogen ( $\text{N}_2$ ), those in  $\text{CH}_4$  were higher order alkanes whilst those in  $\text{CO}_2$  were predominantly  $\text{CO}$  and  $\text{N}_2$ .

**TABLE 2.** Purities of Gases Employed in Study

Gas	He	CH <sub>4</sub>	H <sub>2</sub>	CO <sub>2</sub>	N <sub>2</sub>
Purity <sup>a</sup>	5.0	5.5	5.0	4.5	5.0

<sup>a</sup>Example: 3.5 = 99.95%; 5.0 = 99.9990%.

**TABLE 3.** Binary Adsorption Systems Investigated by the Volumetric–Densimetric Method (VDM)<sup>a</sup>

	CO <sub>2</sub>	CH <sub>4</sub>	H <sub>2</sub>	
CO <sub>2</sub>		20%:80% 48%:52% 78%:22%		293 K
CH <sub>4</sub>	21%:79%		20%:80%	293 K
H <sub>2</sub>		80%:20%		
	333 K	333 K		

<sup>a</sup>Sorbent, AC D47/3 (CarboTech); pressure range,  $p < 2$  MPa; temperature(s), 293 K and 333 K.

## ADSORPTION EQUILIBRIUM DATA

Several adsorption equilibria isotherms of pure gases and binary gas mixtures as measured by the volumetric–densimetric method (VDM) are presented in this section. The absolute masses of all the adsorbed components per unit mass of sorbent are given as a function of the sorptive gas pressure at different temperatures. Experimental uncertainties were ca. three-times the size of the graphical symbols used in the figures. The components of the systems and the ranges of temperatures and pressure employed are specified in Table 3 where the numbers indicate the gas concentrations in adsorption equilibrium in mol%. Equilibration times were ca. 3–7 h for the CO<sub>2</sub>/CH<sub>4</sub> systems and 3 h for the H<sub>2</sub>/CH<sub>4</sub> systems. The data were correlated by a generalized isotherm of the Langmuir type taking the fractal dimension of the internal surface of the carbon into account [see Chapter 7 of Keller and Staudt (2004)]:

*For pure gases*

$$n(p, T) = \alpha^p n_\infty^p(T) \frac{[b^p(T) \cdot p]^{\alpha^p}}{1 + [b^p(T) \cdot p]^{\alpha^p}} + \alpha^s n_\infty^s(T) \frac{[b^s(T) \cdot p]^{\alpha^s}}{1 + [b^s(T) \cdot p]^{\alpha^s}} \quad (24)$$

*For binary gas mixtures*

$$n_i(p, T) = \alpha_i^p n_\infty^p(T) \frac{[b_i^p(T) \cdot p_i]^{\alpha_i^p}}{1 + [b_1^p(T) \cdot p_1]^{\alpha_1^p} + [b_2^p(T) \cdot p_2]^{\alpha_2^p}} + \alpha_i^s n_\infty^s(T) \frac{[b_i^s(T) \cdot p_i]^{\alpha_i^s}}{1 + [b_1^s(T) \cdot p_1]^{\alpha_1^s} + [b_2^s(T) \cdot p_2]^{\alpha_2^s}} \quad i = 1, 2 \quad (25)$$

The following parameters apply in these equations:

$n(p,T)$	number of moles of adsorbate
$\lim_{p \rightarrow \infty} n = \alpha^p n_\infty^p + \alpha^s n_\infty^s$	limiting amount adsorbed for $p \rightarrow \infty$
$\alpha^p, \alpha^s > 0$	characteristic exponents related to the diameter of the adsorbed molecules and the fractal dimension of the sorbent material
$b^r(T) = \frac{1}{p_0} \sqrt{\frac{T_0}{T}} \exp\left(\frac{q^r}{RT}\right)$	Langmuir parameters for adsorption sites of type $r = p, s$
$R = R/M$	specific gas constant

The indices “p” and “s” refer to “primary” and “secondary” adsorption or pore systems, corresponding to meso- and micro-pores.

For gaseous mixtures, where adsorption isotherms (25) apply, the parameters  $\alpha^r, n_\infty^r, q^r, r = p, s$  determined for the pure gas adsorption isotherms via equation (24) can be used. However, in this case, the relative mean deviation ( $f_m$ ) between the predicted ( $n_{PRE}$ ) and measured amounts adsorbed ( $n_{EXP}$ ), i.e.

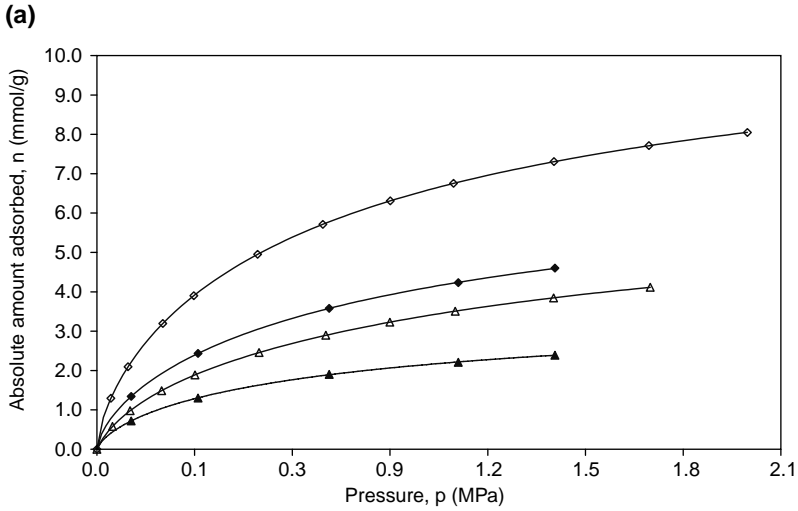
$$f_m = \frac{1}{N} \sum_{i=1}^N \left( |n_{PRE} - n_{EXP}| / n_{EXP} \right)_i \tag{26}$$

and the relative dispersion ( $\sigma$ ) of these data, i.e.

$$\sigma^2 = \frac{1}{N} \sum_{i=1}^N \left( (n_{PRE} - n_{EXP})^2 / n_{EXP}^2 \right)_i \tag{27}$$

are typically of the order of 10% or greater. On the other hand, the experimental data for the co-adsorption equilibria ( $n_{EXP}$ ) can be correlated directly by the isotherms given in equation (25). Under these circumstances, the mean absolute deviation and dispersion between the correlated ( $n_{COR}$ ) and experimental data ( $n_{EXP}$ ), cf. equations (26) and (27), are typically ca. 0.1%. Numerical examples for this situation are given in the schemes below Figures 6–11. As can be seen, the co-adsorption equilibria of  $CO_2/CH_4$  and  $H_2/CH_4$  on AC D47/3 could not be predicted accurately from the pure component adsorption isotherm via the mixture isotherm [equation (25)] but rather had to be determined experimentally (Iossifova 2006).

From the  $f_m/\sigma$  data given in Figures 8–11, it will be seen that the co-adsorption equilibria could not be predicted from pure adsorption isotherms by the model equation (26) if the stronger adsorbed component ( $CO_2$  in Figures 8 and 9 and  $CH_4$  in Figures 10 and 11, respectively) was abundant. This result has been confirmed by the use of other models for mixture adsorption, for example the simple Langmuir AI or the classical IAST theory, cf. Keller and Staudt (2004) and Iossifova (2006). Hence, in the adsorption of gaseous mixtures there is still a need to develop more effective mixture isotherms and to provide more accurate and reliable experimental data of co-adsorption isotherms.



Sorbent	Sorpitive	Temperature and pressure	$f_m/\sigma$			
				$n_{tot}$ (mmol/g)	$n_{CO_2}$ (mmol/g)	$n_{CH_4}$ (mmol/g)
AC D47/3	CO <sub>2</sub> /CH <sub>4</sub> 20.4:79.6 mol%	293 K $p < 1.5$ MPa (five points)	Prediction	1.51E-01	1.30E-01	2.22E-01
				1.57E-01	1.58E-01	2.28E-01
			Correlation	7.52E-04	2.70E-03	3.21E-03
				11.00E-04	3.35E-03	3.60E-03

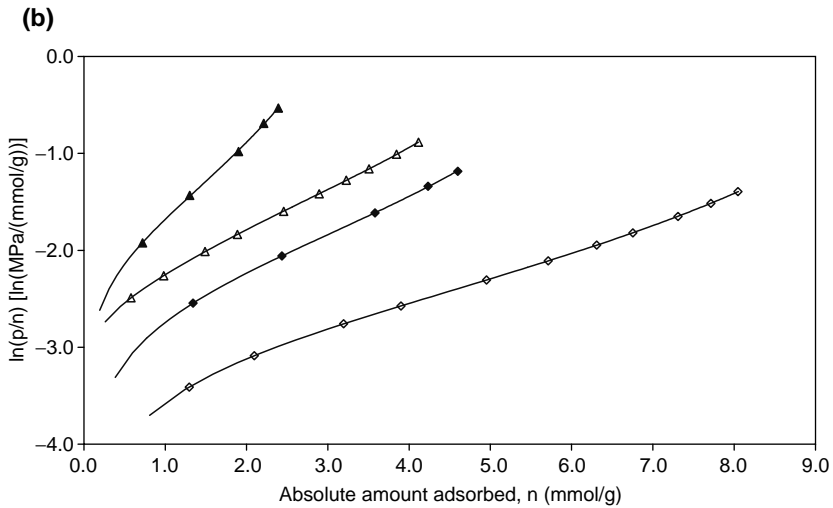
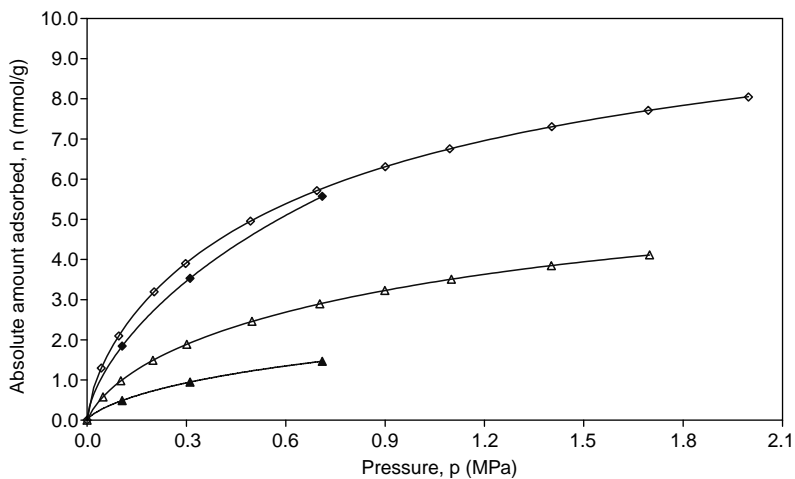
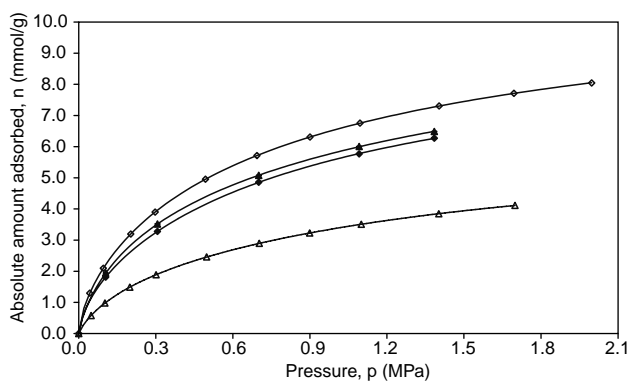


**Figure 6.** Adsorption equilibria of pure CO<sub>2</sub> and CH<sub>4</sub> and of a CO<sub>2</sub>/CH<sub>4</sub> gas mixture ( $y_{CO_2} = 20.4$  mol%,  $y_{CH_4} = 79.6$  mol%) at 293 K on activated carbon AC D47/3. In (a), the statistical uncertainties ( $f_m, \sigma$ ) of the co-adsorption data predicted from the pure adsorption data and correlated via equations (26) and (27), respectively, are given in the scheme. In (b), the quantity  $\ln(p/n)$  is correlated with the absolute amounts adsorbed [cf. equation (19)] of the pure gases (CO<sub>2</sub> ...  $\diamond$ , CH<sub>4</sub> ...  $\triangle$ ), the total amount of the gas mixture adsorbed (CO<sub>2</sub> + CH<sub>4</sub> ...  $\blacklozenge$ ) and the partial amount of methane in the mixture adsorbed (CH<sub>4</sub> ...  $\blacktriangle$ ).



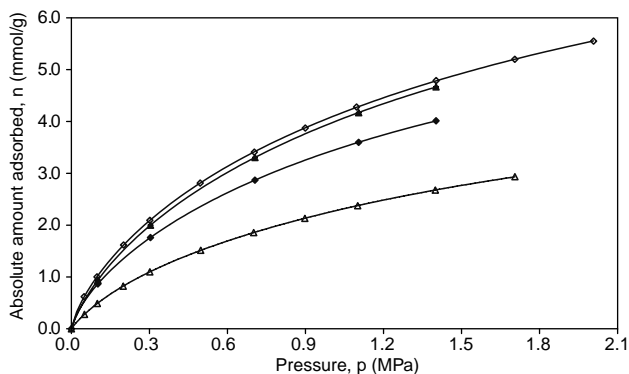
Sorbent	Sorbative	Temperature and pressure		$f_m/\sigma$			
				$n_{\text{tot}}$ (mmol/g)	$n_{\text{CO}_2}$ (mmol/g)	$n_{\text{CH}_4}$ (mmol/g)	
AC	CO <sub>2</sub> /CH <sub>4</sub>	293 K	Prediction	7.43E-02	1.18E-01	1.79E-01	
D47/3	48.3: 51.7 mol%	$p < 1.5$ MPa (three points)		8.79E-02	1.51E-01	1.82E-01	
				Correlation	3.89E-04	2.83E-04	1.15E-04
					4.31E-04	3.21E-04	1.64E-04

**Figure 7.** Adsorption equilibria of pure CO<sub>2</sub> and CH<sub>4</sub> and of a CO<sub>2</sub>/CH<sub>4</sub> gas mixture ( $y_{\text{CO}_2} = 48.3$  mol%,  $y_{\text{CH}_4} = 51.7$  mol%) at 293 K on activated carbon AC D47/3. Statistical uncertainties ( $f_m, \sigma$ ) of co-adsorption data (total and partial loads) predicted from pure adsorption data and correlated via equations (26) and (27), respectively, are given in the scheme. The data points in the figure relate to the absolute amounts adsorbed as follows:  $\diamond$ , pure CO<sub>2</sub>;  $\triangle$ , pure CH<sub>4</sub>;  $\blacklozenge$ , total amount of gas mixture (CO<sub>2</sub> + CH<sub>4</sub>);  $\blacktriangle$ , partial amount of methane.



Sor bent	Sorptive	Temperature and pressure		$f_m/\sigma$		
				$n_{tot}$ (mmol/g)	$n_{CO_2}$ (mmol/g)	$n_{CH_4}$ (mmol/g)
AC D47/3	CO <sub>2</sub> /CH <sub>4</sub> 77.5 / 22.5 mol%	293 K $p < 1.5$ MPa (five points)	Prediction	5.56E-02	6.61E-02	2.65E-00
				6.17E-02	7.87E-02	2.84E-00
			Correlation	6.96E-04	7.29E-04	-
				8.59E-04	9.00E-04	

**Figure 8.** Adsorption equilibria of pure CO<sub>2</sub> and CH<sub>4</sub> and of a CO<sub>2</sub>/CH<sub>4</sub> gas mixture ( $y_{CO_2} = 77.5$  mol%,  $y_{CH_4} = 22.5$  mol%) at 293 K on activated carbon AC D47/3. Statistical uncertainties ( $f_m, \sigma$ ) of co-adsorption data (total and partial loads) predicted from pure adsorption data and correlated via equations (26) and (27), respectively, are given in the scheme. The data points in the figure relate to the absolute amounts adsorbed as follows:  $\diamond$ , pure CO<sub>2</sub>;  $\triangle$ , pure CH<sub>4</sub>;  $\blacktriangle$ , total amount of gas mixture (CO<sub>2</sub> + CH<sub>4</sub>);  $\blacklozenge$ , partial amount of CO<sub>2</sub>. Obviously, the co-adsorption data cannot be predicted from the pure adsorption isotherms by the model equation (26) if the stronger adsorbed component (CO<sub>2</sub>) is abundant.



Sor bent	Sorptive	Temperature and pressure		$f_m/\sigma$		
				$n_{tot}$ (mmol/g)	$n_{CO_2}$ (mmol/g)	$n_{CH_4}$ (mmol/g)
AC D47/3	CO <sub>2</sub> /CH <sub>4</sub> 79.4:20.6 mol%	333 K $p < 1.5$ MPa (five points)	Prediction	2.55E-02	2.22E-02	4.04E-01
				2.85E-02	2.53E-02	4.50E-01
			Correlation	3.53E-04	2.86E-04	3.77E-04
				4.43E-04	2.92E-04	4.49E-04

**Figure 9.** Adsorption equilibria of pure CO<sub>2</sub> and CH<sub>4</sub> and of a CO<sub>2</sub>/CH<sub>4</sub> gas mixture ( $y_{CO_2} = 79.4$  mol%,  $y_{CH_4} = 20.6$  mol%) at 333 K on activated carbon AC D47/3. Statistical uncertainties ( $f_m, \sigma$ ) of co-adsorption data (total and partial loads) predicted from pure adsorption data and correlated via equations (26) and (27), respectively, are given in the scheme. The data points in the figure relate to the absolute amounts adsorbed as follows:  $\diamond$ , pure CO<sub>2</sub>;  $\triangle$ , pure CH<sub>4</sub>;  $\blacktriangle$ , total amount of gas mixture (CO<sub>2</sub> + CH<sub>4</sub>);  $\blacklozenge$ , partial amount of CO<sub>2</sub>.

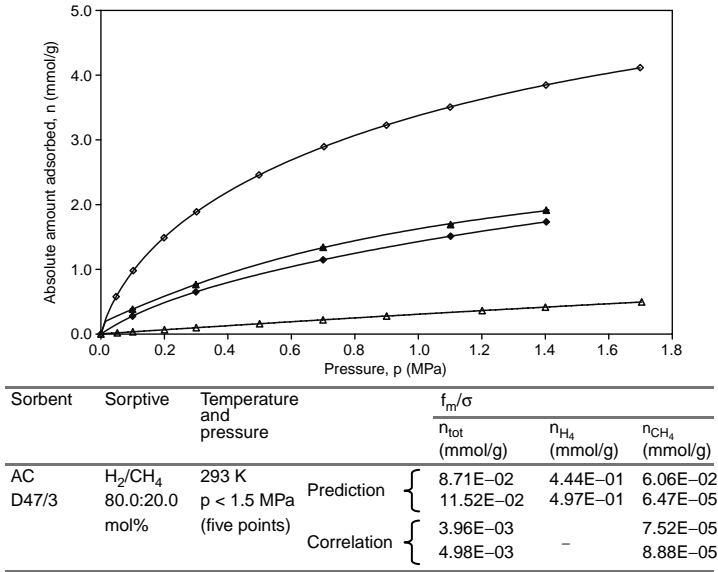


**Figure 10.** Adsorption equilibria of pure H<sub>2</sub> and CH<sub>4</sub> and of an H<sub>2</sub>/CH<sub>4</sub> gas mixture ( $y_{H_2} = 80.0$  mol%,  $y_{CH_4} = 20.0$  mol%) at 293 K on activated carbon AC D47/3. Statistical uncertainties ( $f_m, \sigma$ ) of co-adsorption data (total and partial loads) predicted from pure adsorption data and correlated via equations (26) and (27), respectively, are given in the scheme. The data points in the figure relate to the absolute amounts adsorbed as follows:  $\diamond$ , pure CH<sub>4</sub>;  $\triangle$ , pure H<sub>2</sub>;  $\blacktriangle$ , total amount of gas mixture (H<sub>2</sub> + CH<sub>4</sub>);  $\blacklozenge$ , partial amount of CH<sub>4</sub>.

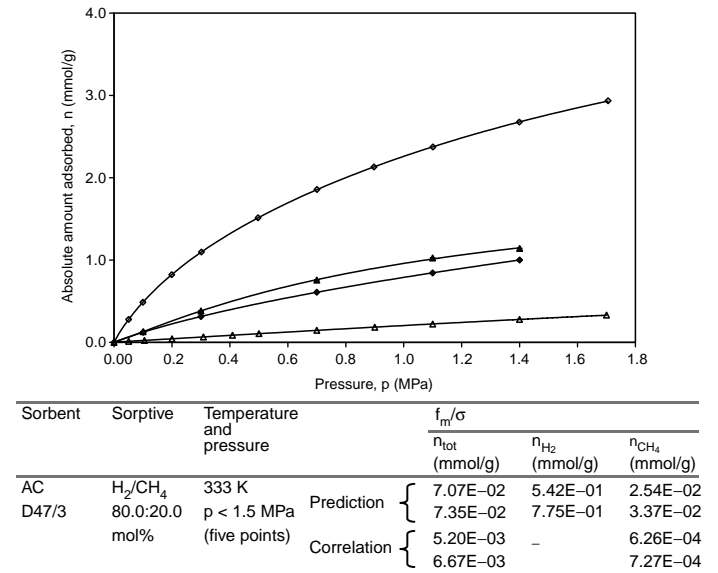


**Figure 11.** Adsorption equilibria of pure H<sub>2</sub> and CH<sub>4</sub> and of an H<sub>2</sub>/CH<sub>4</sub> gas mixture ( $y_{H_2} = 80.0$  mol%,  $y_{CH_4} = 20.0$  mol%) at 333 K on activated carbon AC D47/3. Statistical uncertainties ( $f_m, \sigma$ ) of co-adsorption data (total and partial loads) predicted from pure adsorption data and correlated via equations (26) and (27), respectively, are given in the scheme. The data points in the figure relate to the absolute amounts adsorbed as follows:  $\diamond$ , pure CH<sub>4</sub>;  $\triangle$ , pure H<sub>2</sub>;  $\blacktriangle$ , total amount of gas mixture (H<sub>2</sub> + CH<sub>4</sub>);  $\blacklozenge$ , partial amount of CH<sub>4</sub>.

We sincerely hope that this is considered as a challenge, worthy to be pursued by the younger generation of research workers.

## REFERENCES

- Basmdjian, D. (1996) *The Little Adsorption Book*, CRC Press, Boca Raton, FL, USA.
- Beutekamp, S. (2002) *Adsorptionsgleichgewichte der reinen Gase  $CO_2$ ,  $CH_4$ ,  $N_2$  und deren binären Gemische an verschiedenartigen porösen Stoffen*, Fortschrittberichte VDI, Reihe 3, Verfahrenstechnik, Nr. 736, Düsseldorf, VDI-Verlag, ISBN 3-18-373603-9.
- Iossifova, N. (2006) *Untersuchungen von Gemischgleichgewichten bei adsorptiven Gastrenn- und Reinigungsverfahren*, Fortschrittberichte VDI, Reihe 3, Verfahrenstechnik, VDI-Verlag, Düsseldorf, in preparation.
- Kast, W. (1988) *Adsorption aus der Gasphase*, Verlag Chemie, Weinheim, Germany.
- Keller, J.U., Dreisbach, F., Rave, H., Staudt, R. and Tomalla, M. (1999) *Adsorption* **5**, 199.
- Keller, J.U. and Staudt, R. (2004) *Gas Adsorption Equilibria, Experimental Methods and Adsorption Isotherms*, Kluwer/Springer, Norwell, MA, USA.
- Reid, R.C., Prausnitz, J.M. and Poling, B.E. (1983) *The Properties of Gases and Liquids*, McGraw-Hill, New York.
- Rouquerol, F., Rouquerol, J. and Sing, K.S.W. (1999) *Adsorption by Powders and Porous Solids*, Academic Press, San Diego, CA, USA.
- Ruthven, D.M., Farooq, D. and Knaebel, K.S. (1994) *Pressure Swing Adsorption*, VCH-Wiley, Weinheim/New York.
- Schein, E. (2003) *Research Report DFG Ke 334/23-1*, Institute Fluid- & Thermodynamics, University of Siegen, Siegen, Germany.
- Sengers, J.V., Kayser, R.F., Peters, C.J. and White, Jr., H.F. (Eds) (2000a) *Equations of State for Fluids and Fluid Mixtures, Part I, IUPAC Series in Experimental Thermodynamics*, Vol. V, Elsevier, Amsterdam, The Netherlands.
- Sengers, J.V., Kayser, R.F., Peters, C.J. and White, Jr., H.F. (Eds) (2000b) *Equations of State for Fluids and Fluid Mixtures, Part I, IUPAC Series in Experimental Thermodynamics*, Vol. II, Elsevier, Amsterdam, The Netherlands.
- Staudt, R. (2000) *Habilitationsschrift*, Institute Fluid- & Thermodynamics, University of Siegen, Siegen, Germany.
- van Ness, H.C. (1969) *Ind. Eng. Chem., Fundam.* **8**, 464.
- Yang, R.T. (1997) *Gas Separation by Adsorption Processes*, Imperial College Press, London, UK.
- Yang, R.T. (2003) *Adsorbents, Fundamentals and Applications*, Wiley-Interscience, Hoboken, NJ, USA.